

Electronic states of a substitutional chromium impurity in GaAs

L. A. Hemstreet

Naval Research Laboratory, Washington, DC 20375

J. O. Dimmock

Office of Naval Research, Arlington, Virginia 22217

(Received 2 November 1978)

The $X\alpha$ scattered-wave cluster method has been used to investigate the electronic properties associated with various charge configurations of a substitutional chromium impurity in GaAs. The usual spin-restricted formalism is found to provide an inadequate treatment of the strong electron-electron interactions between the d -like electrons associated with the chromium impurity and leads to a poor description of the resulting electronic states. Two methods of improving the treatment of the impurity electron-electron interactions are proposed and investigated. In the first approach the spin-polarized electronic states of the various clusters are calculated using a spin-unrestricted formalism. This leads to different energy spectra for electrons of different spin and consequently incorporates some of the broad features of the true many-electron multiplet structure in what is essentially a single-electron description. The second approach consists in treating the electron-electron interactions as a perturbation on the single-particle cluster states obtained from the spin-restricted calculations. The many-electron crystal-field term states are then calculated using a modification of the standard crystal-field theory in the strong-field coupling limit. Both of these approaches are applied to the study of the chromium impurity in the Cr^{3+} and Cr^{2+} charge configurations, and the results are compared and discussed.

I. INTRODUCTION

Chromium-doped GaAs has been the object of a great deal of study over the last few years both because of its use as a semi-insulating substrate for epitaxial crystal growth as well as for its potential applications in such devices as the field-effect transistor and photoconductors. Despite these efforts, however, the detailed nature of the electronic properties associated with the chromium impurity are still not well understood. Not only have the energy levels not yet been determined with any great accuracy, but even the number of such levels is in dispute. Experimentally the problem is complicated by the simultaneous presence of other deep-level defects in the samples, as well as by the fact that chromium can exist in several charge states and conversion between such charge states can be induced by the measurement process itself. On the theoretical side the localized nature of the deep chromium acceptor makes the usual effective-masslike theories inapplicable. Beyond this the experimental measurements also indicate strong electron-electron interactions involving the defect electrons and strong Jahn-Teller lattice distortions accompanying the defects, both of which complicate the analysis.

In an effort to gain some further qualitative insight into the nature of the electronic states associated with

a chromium impurity in gallium arsenide, we have used a cluster approach similar to that applied earlier by one of us (L.A.H.) to the study of transition-metal impurities in silicon.¹ Basically, one utilizes the localized nature of the deep defect perturbing potential and focuses only on those host atoms neighboring the defect site. The electronic states of a cluster composed of the impurity plus surrounding host atoms are calculated using a scattered-wave formalism,² coupled with the local $X\alpha$ exchange approximation,³ and the defect-related states are obtained from a direct comparison of these results to those obtained from an analogous calculation on an ideal cluster without the defect.

The plan of this paper is as follows: in Sec. II we present the results of spin-restricted cluster calculations involving various charge states of a substitutional chromium impurity in GaAs. In Sec. III we present two schemes for improving the treatment of the electron-electron interactions between the d -like electrons associated with the transition-metal impurity. In all of these calculations the possible effects due to lattice relaxation accompanying the defect have been neglected. Finally, in Sec. IV, we discuss our results and arrive at certain qualitative conclusions involving the nature of the electronic states associated with the substitutional chromium impurity in GaAs.

II. SPIN-RESTRICTED CLUSTER CALCULATIONS

The calculational scheme is basically the same as that employed previously for the study of transition-metal impurities in silicon.¹ Since chromium is assumed to substitute for gallium in gallium arsenide, the simplest ideal cluster is formed by surrounding a central gallium atom by four arsenic nearest neighbors and twelve hydrogenlike saturators at the positions of the twelve next-nearest-neighbor Ga sites. The whole system is then enclosed by an outer Watson sphere. A charge of $-3e$, where e is the magnitude of the electronic charge, is distributed on the surface of this Watson sphere in order to insure charge neutrality of the cluster as a whole. The corresponding defect cluster is obtained by replacing the central gallium atom by chromium. The total cluster potential is constructed to have the muffin-tin form, with the local $X\alpha$ exchange approximation being used. For simplicity, all muffin-tin spheres are chosen to have the same radius of 2.31 a.u. (taken to be equal to half the GaAs nearest-neighbor distance in bulk GaAs) and the same value³ of $\alpha = 0.706$ is used everywhere except in the chromium sphere, where $\alpha = 0.713$. The electronic states of the system are calculated using the scattered-wave formalism² and all calculations are carried to self-consistency unless otherwise noted. Transition energies are calculated using the standard transition-state procedure.³

The spin-restricted energy-level spectra associated with the various clusters considered in the present investigations are shown in Fig. 1. In all cases the spectra exhibit a set of occupied valence states separated from a set of unoccupied conduction levels by an energy gap which varies in magnitude from roughly 1.25 eV in the ideal case [Fig. 1(a)] to about 1.35 eV in the case of the defect clusters [Figs. 1(b)–1(d)].

In the case of the defect spectra the chromium $3d$ levels are split into states of e and t_2 symmetry by the tetrahedral field of the neighboring host atoms. The t_2 component seems to hybridize with ligand states of the same symmetry, leading to $2t_2$ and $4t_2$ levels with substantial d -like character in both the valence and conduction states, respectively. The e component [labelled $0e$ in Figs. 1(b)–1(d)], on the other hand, is calculated to lie in the gap region of the host spectrum and has an energy separation of approximately 1.10, 1.25, and 0.70 eV from the uppermost occupied valence state in Figs. 1(b)–1(d), respectively. This state is largely d -like in character and has by far the majority of its charge located within the muffin-tin sphere centered on the chromium site. Neutral chromium (Cr^{3+}) corresponds to three electrons in this $0e$ level [Fig. 1(b)], while the various other charge states are obtained by adding (subtracting) electrons to (from) this highly localized state. The spectra of the Cr^{2+} and Cr^{4+} configurations are shown

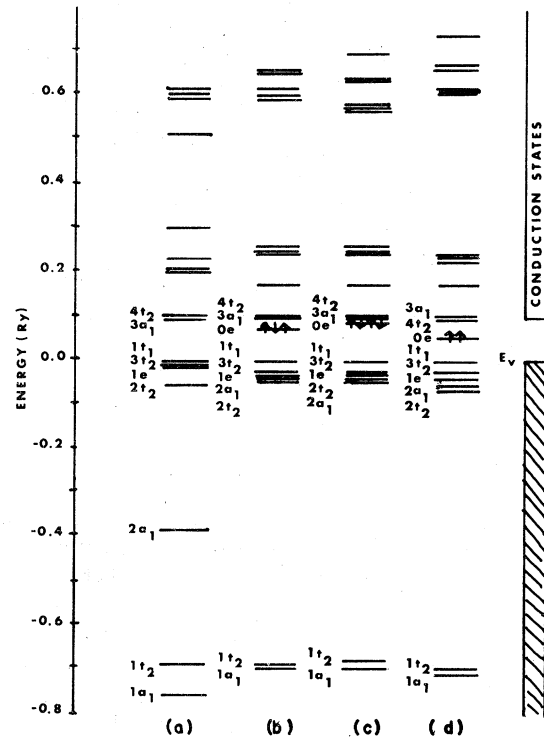


FIG. 1. Calculated spin-restricted energy-level spectra of the clusters representing (a) "ideal" gallium arsenide and gallium arsenide with a substitutional chromium impurity in the configurations (b) Cr^{3+} , (c) Cr^{2+} , and (d) Cr^{4+} .

in Figs. 1(c) and 1(d), and correspond to an occupancy of four and two electrons, respectively.

In addition to the appearance of d -like structure in the defect energy spectra, the only other difference of any consequence between the ideal and defect spectra is the large upward shift of the $2A_1$ level upon replacement of the central gallium atom by chromium. In the ideal case this state is associated with σ bonding between the gallium atom and its four arsenic nearest neighbors. When gallium is replaced by chromium this bonding becomes much weaker because the contribution from the gallium $4s$ electrons is replaced by that of the chromium $4s$ state, which has much higher energy. The σ bonding $2A_1$ level is thus raised in energy when the substitution is made, as shown in Figs. 1(b)–1(d).

One can also obtain information about the charge distribution of the individual cluster eigenstates and/or of the total cluster charge. The self-consistent results for the total charge contained within the various regions of the cluster are shown in Table I for both the ideal cluster and for those containing the Cr^{2+} , Cr^{3+} , and Cr^{4+} configurations of the chromium impurity. It is interesting to note that the total charge contained within the chromium muffin-tin

TABLE I. Calculated total cluster charge distributions for the "ideal" gallium arsenide cluster as well as for the clusters containing a substitutional chromium impurity in the Cr^{3+} , Cr^{2+} , and Cr^{4+} configurations.

Region	Cluster Charge Distributions			
	Ideal Cluster	Cluster with Cr^{3+}	Cluster with Cr^{2+}	Cluster with Cr^{4+}
Central	30.25 e	23.40 e	23.43 e	23.39 e
(4)NN As	31.37	31.36	31.36	31.35
(12)NNN	0.70	0.71	0.76	0.66
Interstitial	7.56	7.44	7.79	7.07
Extramolecular	0.12	0.13	0.16	0.11

sphere remains essentially constant even though the occupancy of the d -like $0e$ level changes from two to four in the sequence Cr^{4+} to Cr^{2+} . Since this state is highly localized at the impurity site, one might expect a significant increase (decrease) in the total chromium charge every time an electron is added to (subtracted from) this level. The fact that this is not observed suggests that the wave functions associated with the occupied valence states of the host must adjust their charge so that the configuration at the impurity site remains essentially neutral or close to it, in agreement with the conclusions of Haldane and Anderson.⁴

Although the interpretation of the available experimental data on the chromium impurity in GaAs is unclear and still somewhat controversial, there does not seem to be much quantitative agreement between any of the experimental results and the present spin-restricted cluster calculations. Not only are the positions of the chromium levels in poor agreement with experiment but even the spins of the ground-state configurations are incorrectly given. The spin-restricted cluster calculations predict spins of $S = 0$ and $S = \frac{1}{2}$ for Cr^{2+} and Cr^{3+} , respectively, while the EPR data⁵⁻⁷ suggests $S = 2$ and $S = \frac{3}{2}$ for the corresponding states. The fact that the EPR data indicates a Hund rule ground state (maximum spin multiplicity) implies that electronic correlation must be an important factor in GaAs:Cr, at least among the d electrons associated with the impurity. Such effects have been ignored in the present spin-restricted calculations, which are based on a single-particle picture with all spin states treated alike. The EPR measurements also suggest strong Jahn-Teller effects which the present theory also neglects. To get even semiquantitative agreement with experiment would seem to require that either or both effects be included. In Sec. III the problem of electronic correlations will be considered using two separate but approximate approaches. The incorporation of lattice distortion into the cluster calculations will be left to a later date.

III. ELECTRON-ELECTRON INTERACTIONS

In this section we describe the results of two attempts to better include the effects of electronic interactions among the d -like electrons associated with the transition-metal chromium impurity in GaAs. In the first approach one repeats the cluster calculations as described previously but employs a spin-unrestricted formalism³ in which electrons with different spin are treated separately. This spin-polarized method leads to different energy spectra for spin-up and spin-down electrons and consequently to the appearance of some of the broad features associated with the many-electron multiplet structure in the one-electron picture.

The second approach essentially consists in treating the electron-electron interactions as a perturbation on the single-particle cluster states, in much the same way that the many electron term values are derived from the single-particle Hartree-Fock states of the atom.⁸ The resulting energy levels are many-electron states and are analogous to the strong-field term values of standard crystal-field theory.⁸⁻¹¹

A. Spin-polarized calculations

Using this approach each spin is treated independently and, since the exchange contribution to the cluster potential depends only on the charge density associated with electrons of parallel spin, electrons with differing spin may experience different potentials. The resulting asymmetry breaks the spin degeneracy of the single-particle states discussed previously and leads to different energy spectra for the spin-up and spin-down levels. In the case of a transition-metal impurity in GaAs, for example, the crystal-field-split e and t_2 d -like components will be separated into e_1 , e_1 , t_{21} and t_{21} states. If the spin splittings of these levels are of the same order of magnitude or larger than the crystal-field splitting the possibility exists that the $4t_{21}$ level will be shifted down below the $0e_1$ level, for example, leading to a

ground-state configuration where all electrons have spin up.

Such spin-polarized calculations have been carried out for the cases of Cr^{2+} and Cr^{3+} in GaAs. In both cases it has been found that the spin splittings of the defect-related levels are of the same order of magnitude or larger than the crystal-field effects. The spin-polarized spectrum for Cr^{3+} is shown in Fig. 2. One finds that the $0e_1$ and $4t_{21}$ states are nearly degenerate, having an energy separation of less than 0.0015 Ry. Thus, although the spin of the calculated ground-state configuration of Cr^{3+} remains $S = \frac{1}{2}$, it is essentially degenerate with a state having spin $S = \frac{3}{2}$, corresponding to the $e_1^2 t_{21}$ configuration. Both levels lie about 0.65 eV above the uppermost occupied valence state. Note that the spin-up and spin-down manifolds of Fig. 2 show very little relative splitting of those valence and conduction states derived primarily from the host atom. The major effect of the spin polarization is to split the two spin

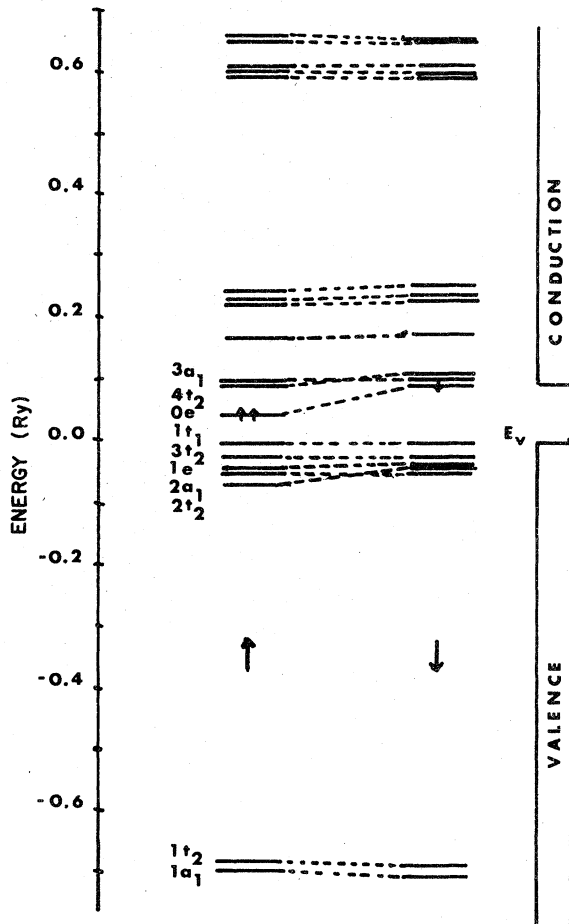


FIG. 2. Calculated spin-polarized energy-level spectrum for a cluster representing gallium arsenide with a substitutional chromium impurity in the Cr^{3+} configuration.

components of the $0e_1$, $2t_2$, and $4t_2$ levels, all of which have strong d -like contributions from the chromium impurity. Moreover, the greater the amount of d character the greater the spin splitting. This indicates that the electron-electron interactions are mainly important among the d electrons.

Similar spin-polarized calculations were attempted for Cr^{2+} . Since the $0e_1$ - $4t_2$ splitting of Fig. 1(c) is only about one half that in Fig. 1(b) (Cr^{3+}), one might expect the $4t_2$ level to be displaced well down below the $0e_1$ level, leading to a ground-state configuration of $e_1^2 t_1^2$ corresponding to $S = 2$. Such a qualitative result is indeed obtained from the spin-polarized calculation for Cr^{2+} in GaAs. However, the self-consistency cycle fails to fully converge in this case. Instead, one finds that the self-consistency procedure converges smoothly only up to a certain point beyond which no further convergence is obtained (i.e., the maximum percentage difference between the cluster potentials for successive iterations no longer decreases but remains approximately constant at about 4%). At the same time the energy spectra of the spin-up and spin-down levels continue to move rigidly apart, with the (minority) spin-down levels being displaced upwards in energy with respect to the (majority) spin-up manifold. This process continues until the uppermost occupied valence state with spin-down (t_{11} symmetry) is displaced above the $4t_2$ level, resulting in an unphysical charge transfer to the impurity. At this point, all spin-up states, including those associated with the host atoms, are split from their spin-down counterparts by large energy differences.

This lack of convergence of the spin-polarized calculation in the case of the high-spin configuration of Cr^{2+} in GaAs is not an isolated event but has been found to occur in the cases of Fe^{3+} and Cr^{3+} ($e_1^2 t_{21}$ configuration) as well. The reasons for this behavior in the case of the high-spin configurations of the transition-metal impurities in GaAs are not presently understood but seem somehow to be related to the relatively small size of the clusters employed in these investigations. The higher-spin configurations have more electrons in the t_{21} state as opposed to the e_1 states. The associated t_{21} wave functions are not as localized or as atomiclike as are those of e_1 but have a substantial mixing of conduction-state character. This results in a larger amplitude in the outer regions of the cluster (i.e., inside the hydrogenlike muffin-tin spheres and in the extra-molecular region) where the total charge densities associated with both spins are by far the smallest (no core charge contributions). Placing extra electrons in the t_{21} level thus has the effect of increasing the spin imbalance in those regions of the cluster where the total charge density is smallest and small fluctuations will therefore have their maximum effect. It is precisely in these regions of the cluster where the source of the convergence diffi-

culties in the spin-polarized calculations is found to be. The choice of larger cluster sizes should de-emphasize the contribution of these regions and smooth the convergence. Follow-up efforts in this direction are presently in progress.

B. Perturbation theory

This approach consists in treating the electron-electron interactions as a perturbation on the single-particle states obtained from the spin-unrestricted cluster calculations of Sec. II. Assuming only interactions among d -like electrons to be significant, the single-particle $0e$ and $4t_2$ levels of Figs. 1(b)–1(d) are used as basis states and all possible terms associated with the configurations $e^n t_2^m$, $n + m = N$, are formed, where N is the total number of d -like electrons associated with the impurity (e.g., $N = 3$ for Cr^{3+} , and 4 for Cr^{2+}). In the absence of the electron-electron interactions all terms derived from a particular configuration $e^n t_2^m$ will be degenerate. The inclusion of such interactions splits this degeneracy and mixes the states.

This procedure is analogous to the standard strong-field limit of crystal-field theory.⁸ However, the usual theory must be modified to account for the fact that the $0e$ and $4t_2$ basis states are not purely d -like functions localized at the impurity site but rather are true cluster wave functions that have only partial d character and extend throughout the cluster. This is accomplished by introducing the parameters R_{ee} , R_u , and R_{et} , where R_{ee} (R_u) is equal to the fraction of d -like charge that is associated with the $0e$ ($4t_2$) state and which is contained within the impurity muffin-tin sphere. R_{et} is taken to be equal to the geometric mean of R_{ee} and R_u [$R_{et} = (R_{ee} R_u)^{1/2}$]. These parameters, which are obtained directly from the results of the spin-restricted cluster calculations, are then used to scale the various $e-e$, $e-t_2$, and t_2-t_2 electrostatic interaction integrals that appear in the usual version of crystal-field theory.^{8–11} This approach includes only those correlations between d electrons that occur within the impurity sphere and hence probably underestimates the magnitude of the effect somewhat. However, since the spin-polarized calculations for Cr^{3+} indicate that such electron-electron interactions occur mainly among the d electrons, it is expected that the most significant parts of the interaction have been accounted for by the present approach. A brief description of the procedure is given in the Appendix, while a more detailed exposition will be published elsewhere.

The values of the (unscaled) electron-electron-interaction integrals can be approximately expressed in terms of the usual Racah parameters⁸ A , B , and C . Since both the present cluster calculations and the work of Haldane and Anderson⁴ indicate that the

charge density within the chromium core remains that of the free neutral-chromium atom, the values of B and C appropriate to neutral chromium have been taken for Appendix 6 of Ref. 8. These have been determined by fitting the spectrum of the free atom.

In calculating the effects of the electron-electron interactions one must take into account the fact that the average exchange and Coulomb interaction energies have already been included in the central field approximation which forms the starting point for the single-electron spin-restricted calculations. One can express the average interaction energy of all d^N electron configurations in terms of the Racah parameters A , B , and C by the following simple formula (see Appendix 2 of Ref. 8):

$$E = \frac{1}{2}(N-1)N \left[A - \frac{14B}{9} + \frac{7C}{9} \right] \quad (1)$$

The fact that this average energy is already included in the spin-restricted cluster calculations is accounted for in an approximate way by setting $E = 0$ in the perturbation and solving for A , using the already determined values of B and C . The actual values of A , B , and C used in this work are listed in Table II for convenience. Also listed are the values of R_{ee} , R_u , and Δ [the energy difference between the d -like $0e$ and $4t_2$ states of Figs. 1(b)–1(d)] determined from the spin-restricted cluster calculations of Sec. II. It should be noted that no further parameters remain to be determined.

The formalism just described has been applied to the cases of Cr^{3+} and Cr^{2+} in GaAs. The calculated multiplet structures associated with Cr^{3+} and Cr^{2+} , obtained using the parameters listed in Table II, are shown in Figs. 3 and 4, respectively. For Cr^{3+} one calculates a ground state with symmetry 2E ($S = \frac{1}{2}$) with a state of 4T_1 symmetry ($S = \frac{3}{2}$) lying just slightly higher in energy (< 0.020 eV). This near degeneracy is precisely analogous to the result obtained

TABLE II. Values of the parameters Δ , R_{ee} , R_u , A , B , C used in the present calculations of the crystal-field term energies of Cr^{3+} and Cr^{2+} in GaAs.

Parameter	Cr^{3+}	Cr^{2+}
Δ	0.50 eV	0.27 eV
R_{ee}	0.63	0.63
R_u	0.21	0.21
A	-0.090 eV	-0.090 eV
B	0.098 eV	0.098 eV
C	0.312 eV	0.312 eV

from the spin-polarized cluster calculation discussed previously, especially in view of the fact that the 2E and 4T_1 terms are associated with the $e_g^2e_g$ and $e_g^2t_{2g}$ single-electron configurations, respectively. The ordering of the two levels is different from that observed experimentally,⁵ but the small energy difference involved is clearly beyond the accuracy of the present calculations. Furthermore, this ordering can easily be reversed by changing the input parameters only slightly, as will be discussed later.

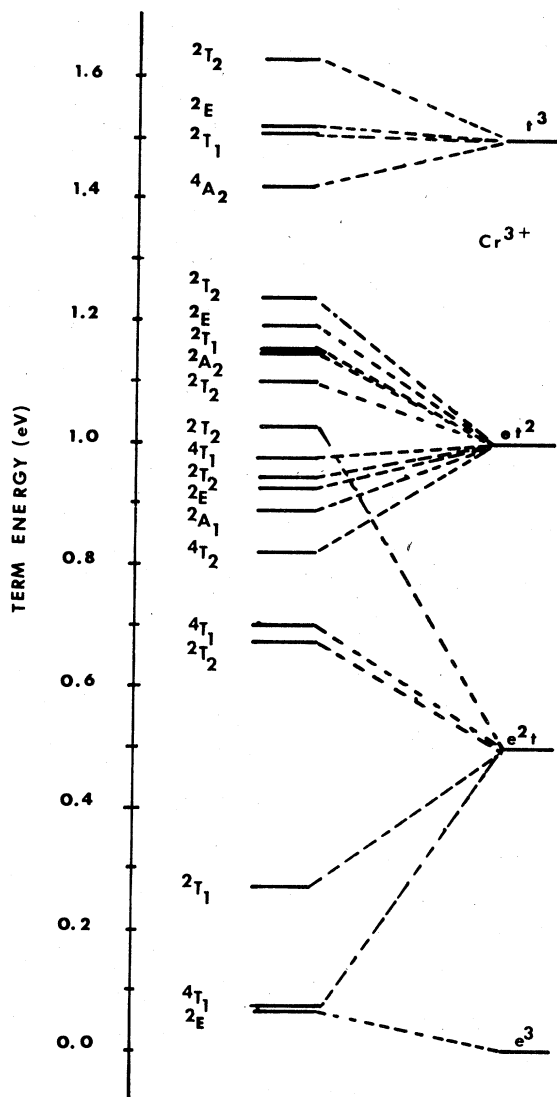


FIG. 3. Crystal-field term energies of Cr^{3+} in gallium arsenide. This spectrum was calculated using the parameters listed in Table II.

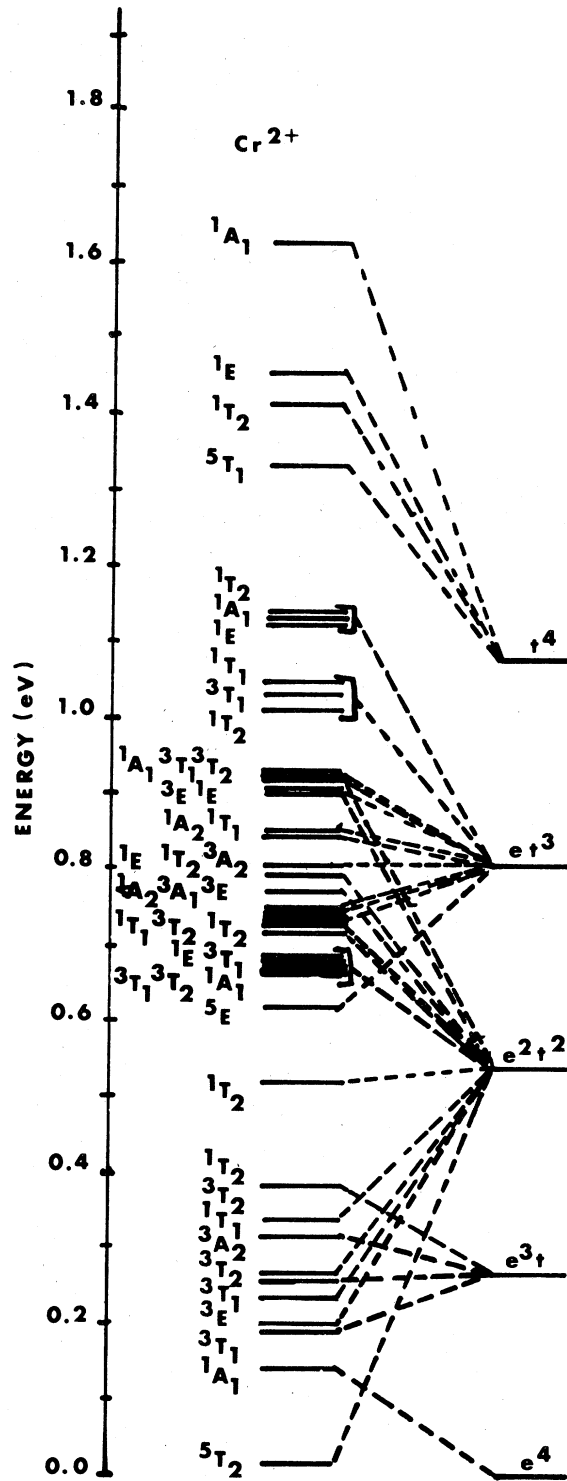


FIG. 4. Crystal-field term energies of Cr^{2+} in gallium arsenide. This spectrum was calculated using the values of the parameters listed in Table II.

In the case of Cr^{2+} the ground-state configuration is unambiguously calculated to have 5T_2 ($S=2$) symmetry. Since this term value is associated with the $e^2t_{2g}^2$ single-electron configuration this result is at least in qualitative agreement with the corresponding spin-polarized cluster calculation, despite the lack of convergence of the latter.

In addition to information about the ground state of the chromium impurity the formalism also provides the energies of internal transitions between the ground state and various excited states. For example, assuming the proper ground state of Cr^{3+} to be the experimentally observed $S = \frac{3}{2}$ configuration, the first spin-allowed transition to an excited state is the 4T_1 - 4T_2 transition of energy 0.75 eV. Slightly higher in energy is the 4T_1 - 4T_1 transition of energy 0.90 eV. Similarly, the 5T_2 - 5E transition of energy 0.65 eV is the first spin-allowed transition from the ground state of Cr^{2+} .

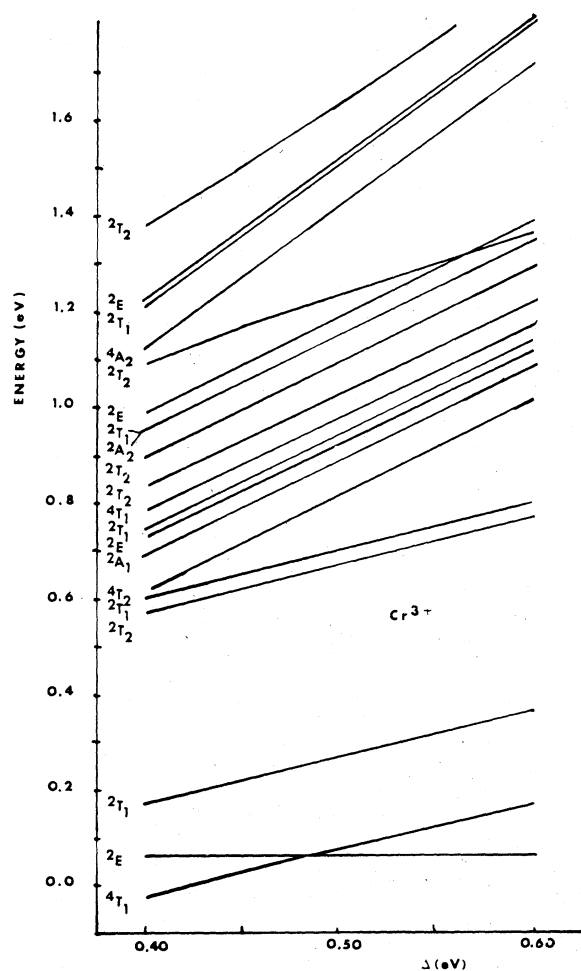


FIG. 5. Plot of the energies of the crystal-field term states of Cr^{3+} as a function of the parameter Δ .

Of course one should not put too much reliance on the precise values of these energies, given the nature of the uncertainties involved. Even ignoring the approximate nature of the formalism itself, the quantitative results are still dependent on the particular choice of parameters A , B , C , Δ , R_{ee} , and R_{tt} . In light of the other approximations involved, fixing B and C by fitting atomic spectra and choosing A to satisfy Eq. (1) seems to be as reasonable a way to proceed as any. Since these parameters are determined primarily on atomic considerations this leaves only the parameters Δ , R_{ee} , and R_{tt} to describe the impurity/host interactions.

The effects of possible variations in the values of these parameters on the term energies of Cr^{3+} are indicated in Figs. 5 and 6. Figure 5 shows the change

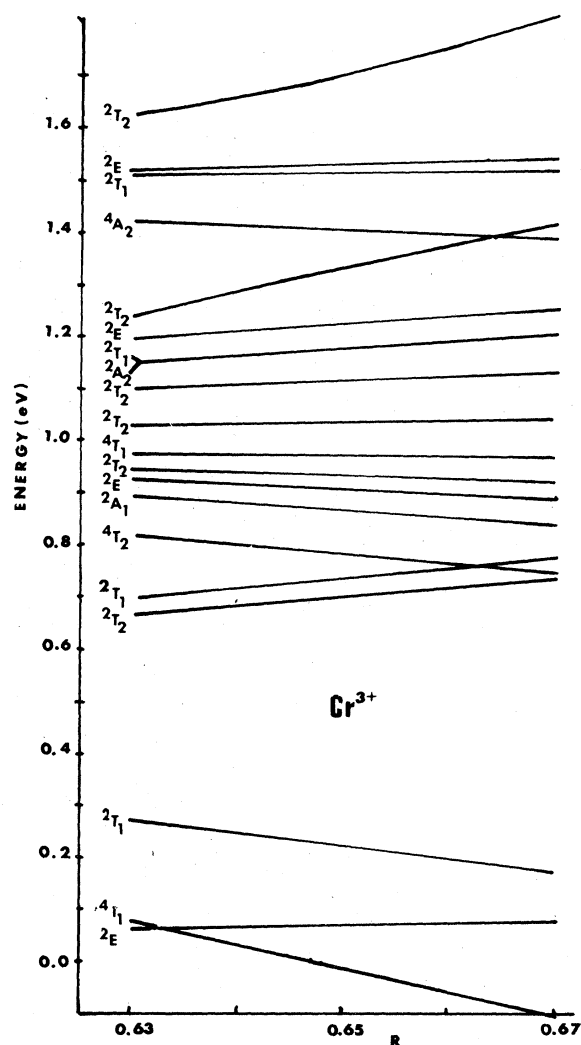


FIG. 6. Plot of the energies of the Cr^{3+} crystal-field term states as a function of R , where $R = R_{ee} = 3R_{tt}$ and R_{ee} , R_{tt} are defined in the text.

in term energies as Δ is varied by approximately $\pm 20\%$ about the calculated value listed in Table II. Since the listed values of R_{ee} and R_{tt} are believed to represent lower bounds on these parameters, Fig. 6 shows how the Cr^{3+} term energies vary as both R_{ee} and R_{tt} are increased by approximately 20% over the calculated values. In the latter figure the energies are plotted as a function of $R = R_{ee}$ and the ratio $R_{ee} = 3R_{tt}$ is maintained throughout.

As can be seen from Figs. 5 and 6, most of the term energies seem to vary reasonably linearly with both Δ and R over the indicated ranges, with changes in Δ generally having a significantly greater effect. With a few exceptions the R dependence of most of the Cr^{3+} term energies tends to be weak. This is encouraging since R seems to be the parameter that is most difficult to estimate accurately. Among several notable exceptions to this trend, however, is the lowest-lying 4T_1 term, which decreases in energy by almost 0.18 eV as R is increased from 0.63 to 0.75. By contrast, the lowest 2E term state, calculated to be the ground state using the parameters of Table II, shows almost no dependence on R . As a result of this behavior the relative ordering of these two states can be reversed by only a slight increase in R , as shown in Fig. 6.

The Δ dependence of the Cr^{3+} term energies can easily be understood by noting that the crystal-field interaction is diagonal in the strong-field-coupling scheme. As a result all term states associated with a particular configuration $e^n t_2^m$ should vary linearly (to a first approximation) as a function of Δ with a slope equal to the value of m . The term states of Fig. 5 should therefore be characterizable by the values of their slope and, indeed, all are clearly one of four types corresponding to the four possible configurations $e^{3-m} t_2^m$, $m = 0, 1, 2, 3$. In particular, the lowest-lying 2E term comes from the e^3 configuration and shows no Δ dependence, while the lowest-lying 4T_1 state varies linearly with a slope of one. The 4T_1 term thus varies with both Δ and R , while the 2E level shows only a weak dependence on R , and the relative ordering of these two levels is very sensitive to the choice of these two parameters. Small changes in either Δ or R reverse the ordering from that calculated using the parameters of Table II, yielding a 4T_1 ground state instead of a 2E ground state. However, regardless of the actual ordering of these two levels, their energy difference should remain small (≤ 0.05 eV) even for reasonably large ($\sim 10\%$) changes in the values of Δ and/or R .

Similar results are obtained for the R and Δ dependence of the term energies of Cr^{2+} . Most of the term energies tend to show only a weak dependence on R , while all the energies vary (approximately) linearly with Δ and have a slope equal to the value of m determined by the configuration $e^{4-m} t_2^m$ from which they are derived. In particular, the 5T_2 ground state

is found to decrease (increase) linearly with R (Δ) with a slope of approximately one, while the lowest-lying 1A_1 term has only a very weak dependence on R . Even though the relative difference between these two energies depends quantitatively on the choice of Δ and R , there is no ambiguity in their ordering as the relative energy separation obtained using the parameters of Table II is sufficiently large to begin with. The 5T_2 level remains the ground state of the system over the entire ranges $0.17 \leq \Delta \leq 0.37$ and $0.63 \leq R \leq 0.75$ considered in our investigations.

IV. DISCUSSION AND CONCLUSIONS

Although perhaps only semiquantitative in nature, the calculations just described clearly indicate the importance of a more careful treatment of the electron-electron interactions between the d -like electrons associated with the chromium impurity in GaAs than is afforded by the spin-restricted cluster formalism. Two different approaches have been investigated, each of which has both advantages and drawbacks. The perturbative scheme of Sec. III B is reasonably straightforward to implement and does yield the full many-electron multiplet structure associated with the impurity, although it does not position this structure with respect to the allowed energy states of the host material. However, one must specify at least six parameters ($A, B, C, \Delta, R_{ee}, R_{tt}$) in order to carry out the calculations, and the quantitative details of the resulting multiplet structure are somewhat dependent on this choice. Three of these (Δ, R_{ee}, R_{tt}) can be determined directly from the results of a spin-restricted cluster calculation, for example, and the Racah parameters B and C can be obtained quite adequately by fitting experimental atomic data. The calculated spectra are not particularly sensitive to the choice of either B or C and the dependence on Δ, R_{ee} , and R_{tt} has already been discussed. This leaves the Racah parameter A still to be specified.

The selection of A is not an entirely trivial matter. In contrast to the standard version of crystal-field theory, a change in the value of A in the present formalism does not lead merely to a rigid displacement of the entire multiplet spectrum as a whole but also changes the relative separations of the various term energies with respect to one another. The reason for this is that A now appears multiplied by varying factors of R_{ee}^2, R_{tt}^2 , and/or R_{et}^2 along the diagonals of the various term matrices. Since $R_{ee}^2 > R_{et}^2 > R_{tt}^2$ in the present case, the various term energies are displaced by differing amounts dependent upon the relative importance of the $e-e$, t_2-t_2 , and $e-t_2$ interactions. The quantitative details of the resulting multiplet structure therefore depend rather strongly on the choice of A . We have chosen A so that in the perturbation the average electronic interaction energy of the d^N

configuration is ignored, arguing that this contribution has already been included in the central-field approximation from which the single-electron properties are calculated. This choice of A seems to us to be physically reasonable and is consistent with the approximations made in choosing B and C .

The spin-polarized cluster calculations, on the other hand, require neither additional parameters nor external input and they entail little more effort than the spin-restricted cluster calculations. But they are also incapable of reproducing the full details of the many-electron multiplet structure. Since there is no one-to-one correspondence between the single-particle defect levels of the cluster calculation and the multi-electron term states, one can only relate the energies of the single-electron transitions to averages over transitions between multiplets. The $0e_1-4t_{21}$ transition energy associated with Cr^{3+} , for example, corresponds to the arithmetic average of the energies of the ${}^4T_1-{}^4T_1$ and ${}^4T_1-{}^4T_2$ multiplet transitions, and other single-particle transition energies involve even more complicated averages over multiplet transitions. Despite this drawback the spin-polarized calculations do describe the broad features of the many-electron defect structure, at least in principle, and furthermore they provide both an approximate single-electron description of defect-related processes as well as a rough placement of the defect spectrum with respect to the allowed energy states of the host material. Both of these latter features often turn out to be quite helpful in the interpretation of available experimental data. Of course, these comments apply only to properly converged spin-polarized calculations of the type described in Sec. III A for Cr^{3+} . As noted earlier, similar spin-polarized cluster calculations involving the high-spin configurations of transition-metal impurities in GaAs did not properly converge and thus only limited information involving either spin-up or spin-down states separately can be obtained in these cases.

Irrespective of their detailed differences, each of the approaches discussed in Sec. II seems to provide the same qualitative picture of a substitutional chromium impurity in gallium arsenide. Both predict a near degeneracy of the $S = \frac{1}{2}$ and $S = \frac{3}{2}$ ground-state energies of Cr^{3+} and both yield a Hund-like ground state ($S = 2$) for Cr^{2+} . Both schemes indicate that spin-allowed internal transitions from the ground state to the lowest-lying excited state should be in the energy range of 0.60–0.90 eV for the combined cases of Cr^{3+} and Cr^{2+} in GaAs. Finally, both approaches indicate that neither the chromium ground state nor the excited states of the same spin are isolated in energy but are in fact nested among terms of differing spin and/or symmetry with similar energies. This indicates a great complexity of defect structure within the band gap of the host material.

Experimentally, photoluminescence,^{12–15} absorp-

tion,¹⁶ photoconductivity,^{17–19} and electron-spin-resonance^{5–7} (ESR) measurements have been carried out on chromium-doped GaAs by various groups. The interpretation of these results is severely complicated by several factors. First, other deep level defects such as oxygen are usually also present in the samples.^{13,16,17} Further, several charge states of the chromium impurity are often present in the same sample at the same time, and transitions between such charge states can be photoinduced.^{5–7} Finally, strong Jahn-Teller distortions are known to accompany the Cr^{2+} and Cr^{3+} states of chromium.^{5,6} Despite these complications, several chromium-related features of the measurements have been isolated: the photoluminescence peaks observed near 0.57 and 0.84 eV are attributed to the presence of chromium^{13,15} as are peaks in the photoconductivity and absorption spectra near 0.90 eV.^{16–18} All but the 0.57 eV peak in the luminescence spectrum are thought to be correlated with the Cr^{2+} charge state, but there is still some controversy over the identification of the initial and final states of the transitions associated with the rest of the peaks.^{7,13,14,20} It is now generally well accepted, however, that the 0.84 eV zero-phonon line in the luminescence spectrum can be assigned to an intracenter transition involving the ground state of Cr^{2+} and the first excited state of the same spin. In Fig. 4 this would correspond to the ${}^5T_2-{}^5E$ transition, which was calculated to have an energy of 0.65 eV in Sec. III B. While not in exact agreement with experiment, this result is a substantial improvement over the value of 0.27 eV that one would obtain using the spin-restricted single-electron formalism of Sec. II.

Of course, the present calculations do not include any effects due to the Jahn-Teller induced lattice distortion that is known to accompany the Cr^{2+} impurity in GaAs, and so it is not really possible to evaluate the theory via a direct comparison to experiment. In order to compare the two results one should either include the effects of lattice relaxation in the theory or one should remove them from the experiment. We are presently planning to do the former by incorporating lattice distortions of the correct symmetry into the cluster calculations and calculating the resulting changes in the electronic states of Cr^{2+} as a function of the distortion. Very recently, however, Krebs and Stauss²¹ have taken the opposite approach and have independently determined the Jahn-Teller splittings of the Cr^{2+} states by carrying out low-temperature applied stress experiments. At low temperatures there are equal numbers of Cr^{2+} centers along each of the $\langle 100 \rangle$ directions of GaAs. By applying stress along different directions and monitoring population changes of the various centers, Krebs and Stauss are able to determine the energy of the Jahn-Teller splitting of the Cr^{2+} defect states. From this they can determine a value of the ${}^5T_2-{}^5E$ transi-

tion energy in the absence of such splitting. They claim that the best fit to their experimental data is found when the unrelaxed 5T_2 - 5E energy separation is taken to be 0.68 eV. This is in excellent agreement with the value of 0.65 eV determined quite independently in Sec. III B. This value of the 5T_2 - 5E transition energy, when coupled with the magnitude of the Jahn-Teller splitting determined by Krebs and Stauss, also could explain the peak in the optical absorption at around 0.90 eV. These results therefore offer some encouragement that the present formalism will be capable of providing at least a semiquantitative description of the deep level problem in gallium arsenide and other III-V semiconductors.

ACKNOWLEDGMENTS

The authors are happy to acknowledge many stimulating discussions with colleagues at the Naval Research Laboratory, especially Dr. J. J. Krebs and Dr. Bruce D. McCombe. This work was supported in part by the U. S. ONR Contract No. NR322-053.

APPENDIX

In this section we briefly describe our modifications of the standard version of crystal-field theory.⁸⁻¹¹ Since we expect the electrostatic and crystal potential energies to be comparable we operate in the intermediate-field limit and treat both interactions simultaneously. Proceeding in the usual way, employing the strong-field coupling scheme, we choose the single-particle $0e$ and $4t_2$ states described in Sec. II and form all possible configurations $e^n t_2^m$, where $n + m = N$ is the total number of d -like electrons to be distributed among the two levels. With each configuration are associated several crystal term states, the symmetry and spin of which can be determined using standard group theoretical methods (see Table A25 of Ref. 8 for a useful compilation). The allowed term states associated with the various configurations of d^3 , for example, are given as follows:

$$\begin{aligned} e^3: & {}^2E, \\ e^2 t_2: & {}^4T_1 + 2^2T_1 + 2^2T_2, \\ e t_2^2: & {}^4T_1 + 4T_2 + 2A_1 + 2A_2 + 2^2E + 2^2T_1 + 2^2T_2, \\ t_2^3: & {}^4A_2 + 2^2E + 2^2T_1 + 2^2T_2. \end{aligned} \quad (\text{A1})$$

In the absence of both the electron-electron and crystal-field interactions the energies of all the crystal term states will be degenerate. The crystal-field interaction, which is diagonal in the strong-field coupling scheme, serves to split the degeneracy of those terms associated with different configurations, while

the electron-electron interaction splits the degeneracy of the terms within a given configuration.

The crystal-field term energies are obtained by diagonalizing a matrix whose elements are found by taking the matrix elements of the crystal-field and electron-electron interaction operators between the state vectors associated with the various crystal-field term states. Because neither operator has matrix elements between terms of different symmetry the energies associated with such terms can be obtained independently. Since the electron-electron operator does connect terms of the same symmetry (but originating from different configurations) the term energies of a given symmetry must be obtained by diagonalizing a matrix of dimension equal to the number of times that the particular term state appears in the various configurations under consideration. Again using the d^3 configuration as an example, the 2E crystal term state appears four times in Eq. (A1) and hence one must diagonalize a 4×4 matrix to obtain the corresponding term energies.

The effect of the crystal-field interaction is accounted for by adding a factor of $m\Delta$, where Δ is the calculated splitting between the $0e$ and $4t_2$ levels as discussed in Sec. II, to each of the diagonal matrix elements involving a term associated with the $e^n t_2^m$ configuration. The matrix elements of the electrostatic interaction can be calculated using the state vectors given in either Ref. 8 or 9. In either case, all of the matrix elements are expressible as linear combinations of the various electrostatic interaction integrals.

$$\langle ab | g | cd \rangle \equiv \int \int a(1) b(2) \frac{2}{r_{12}} c(1) d(2) d\tau_1 d\tau_2, \quad (\text{A2})$$

where a, b, c, d all belong to the set $\{\zeta, \eta, \xi, \phi, \epsilon\}$ and (ξ, η, ζ) , (ϕ, ϵ) are the components of the threefold $4t_2$ and doubly degenerate $0e$ single-particle states, respectively. There are ten independent matrix elements of the form (A2) if one assumes only that the states $\{\zeta, \eta, \xi, \epsilon, \phi\}$ transform like irreducible representations of T_d . However, if it is further assumed that these states transform like the components of d functions, one can express all of these ten integrals in terms of the three Racah parameters A , B , and C . This is the approximation commonly made in crystal-field theory and we follow the same procedure here.

In an attempt to correct for the fact that our single-particle basis states are not purely d -like, we scale the electrostatic interaction integrals (A2) by introducing the parameters R_{ee} , R_u , and R_{et} described in Sec. III B. If states a and c are both components of $4t_2$ ($0e$), for example, we multiply the product $a(1)c(1)$ by the factor R_u (R_{ee}), which represents the d -like fraction of the $4t_2$ ($0e$) state that is con-

tained within the impurity muffin-tin sphere. If the single-particle states a and c are of mixed symmetry, the product $a(1)c(1)$ is scaled by a factor of $R_{et} = (R_{ee}R_{tt})^{1/2}$. Similar considerations apply to the product $b(2)d(2)$. The net result is that all such interaction integrals of the form $\langle ab|g|cd \rangle$ are scaled by factors of R_{ee}^2 , R_{tt}^2 , $R_{et}R_{tt}$, or $R_{et}^2 = R_{ee}R_{tt}$. This scaling leads, in turn, to different expressions in terms of the Racah parameters for the matrix elements of the electron-electron interaction operator. For example, in the case of $N = 3$ (i.e., Cr^{3+}) the en-

ergy of the 4T_2 term, which appears only once in Eq. (A1), is given by the following matrix element in the standard theory (Table A28, Ref. 8):

$$E({}^4T_2) = 3A - 15B + 2\Delta \quad (\text{A3})$$

Using the present modification this becomes

$$E({}^4T_2) = (A - 5B)R_{tt}^2 + (2A - 10B)R_{et}^2 + 2\Delta \quad (\text{A4})$$

Similarly, the matrix elements associated with the 4T_1 terms are given by the following 2×2 matrix:

$$\begin{matrix} {}^4T_1 & & e^2({}^3A_2)t_2 \\ et_2^2({}^3T_1) & \left(\begin{array}{cc} et_2^2({}^3T_1) & e^2({}^3A_2)t_2 \\ (A - 5B)R_{tt}^2 + (2A + 2B)R_{et}^2 + 2\Delta & 6BR_{et}R_{tt} \\ 6BR_{et}R_{tt} & (A - 8B)R_{ee}^2 + (2A - 4B)R_{et}^2 + \Delta \end{array} \right) \\ e^2({}^3A_2)t_2 & & \end{matrix}$$

Similar modifications occur in the matrix elements associated with other symmetries. Of course, in the limit that $R_{ee} = R_{tt} = R_{et} = 1$ the modified matrix elements all reduce to the standard result.

¹L. A. Hemstreet, Phys. Rev. B 15, 834 (1977).

²K. H. Johnson and F. C. Smith, Jr., Phys. Rev. B 5, 831 (1972).

³J. C. Slater, *The Self-Consistent Field for Molecules and Solids* (McGraw-Hill, New York, 1974).

⁴F. D. Haldane and P. W. Anderson, Phys. Rev. B 13, 2553 (1976).

⁵J. J. Krebs and G. H. Stauss, Phys. Rev. B 15, 17 (1977).

⁶J. J. Krebs and G. H. Stauss, Phys. Rev. B 16, 971 (1977).

⁷U. Kaufmann and J. Schneider, Solid State Commun. 20, 143 (1976).

⁸J. S. Griffith, *The Theory of Transition-Metal Ions* (Cambridge University, Cambridge, 1961).

⁹H. Watanabe, *Operator Methods in Ligand Field Theory* (Prentice-Hall, Englewood Cliffs, 1966).

¹⁰D. S. McClure, in *Solid State Physics*, edited by F. Seitz and

D. Turnbull (Academic, New York, 1959), Vol. 9, p. 400.

¹¹M. D. Sturge, in Ref. 10, Vol. 20, p. 91.

¹²T. Instone and L. Eaves, J. Phys. C. 11, L771 (1978).

¹³W. H. Koschel, S. A. Bishop, and B. D. McCombe, Solid State Commun. 19, 521 (1976).

¹⁴H. J. Stocker and Martin Schmidt, J. Appl. Phys. 47, 2450 (1976).

¹⁵K. Kocott and G. L. Pearson, Solid State Commun. 25, 113 (1978).

¹⁶D. Bois and P. Pinard, Phys. Rev. B 9, 4171 (1974).

¹⁷A. L. Lin and R. H. Bube, J. Appl. Phys. 47, 1859 (1976).

¹⁸H. J. Stocker, J. Appl. Phys. 48, 4583 (1977).

¹⁹D. C. Look, Solid State Commun. 24, 825 (1977).

²⁰U. Kaufmann and W. H. Koschel, Phys. Rev. B 17, 2081 (1978).

²¹J. J. Krebs and G. H. Stauss (unpublished).